NEAR-FIELD BEAMFORMING FOR MU-MIMO MILLIMETER WAVE COMMUNICATION SYSTEM

Gerald C. Nwalozie, Damir Rakhimov, and Martin Haardt

Communications Research Laboratory, Ilmenau University of Technology,
P. O. Box 100565, D-98684 Ilmenau, Germany
Email: {gerald-chetachi.nwalozie, damir.rakhimov, martin.haardt}@tu-ilmenau.de

ABSTRACT

Employing a large number of antennas in conjunction with the exploitation of higher frequencies is a promising solution for improving the rate of future wireless systems. The use of large antenna arrays with high transmission frequencies results in the devices operating in the near-field region of the large-scale antenna arrays. This paper studies near-field beamforming for a multi-user multiple-input multiple-output (MU-MIMO) millimeter wave (mmWave) communication system. We exploit the distance discrimination potentials of the near-field beamforming to facilitate an efficient deployment of high-rate multi-user downlink MIMO mmWave systems. To this end, we study the performance of the near-field beamforming using several precoding schemes. Our numerical results demonstrate a significant performance improvement due to the capability of the near-field beamforming to support reliable communications even for devices that are located at the same angular direction which corresponds to the "worst case" situation.

Index Terms— Near-field beamforming, millimeter wave, MIMO communication.

1. INTRODUCTION

Massive multiple-input-multiple-output (MIMO) and millimeter wave (mmWave) communications have emerged as two key technologies to meet the demands of higher data rates in future wireless systems [1]. Due to the propagation characteristics at mmWave frequencies, base stations (BSs) operating in these high-frequency bands will be equipped with large antenna arrays [2] The resulting effect of the combination of large-scale antennas with high transmission frequencies often causes the communicating devices to operate in the near-field (Fresnel) region of the BS antenna. Hence, the far-field assumption often used for conventional wireless systems does not hold. Radiative near-field propagation takes place between the Fraunhofer distance and the Fresnel distance of large-scale antennas operating at mmWave frequencies [3, 4]. The near-field distance can be several dozen of meters for relatively small antennas operating at mmWave and terahertz (THz) frequencies [5].

The distinction between plane waves and spherical waves is due to the distance between the antenna array and the user location. Within the radiative near-field region, the wavefronts become spherical and exploitation of these spherical wavefronts results in flexible transmit beamforming capabilities. The authors in [6] considered near-field communication for a point-to-point short-range multiple-input multiple-output (MIMO) communication system, which consists of two identical transceiver array antennas that face each other with a distance comparable to the size of the antenna aperture. In [7, 8], near-field communication was considered for antennas based on large intelligent surfaces (LISs) whose large aperture gives rise to operations in the near-field. In particular, in [7], the authors studied a two-user uplink scenario in which the BS is equipped with a LIS. The work studied ideal antenna architectures, where the transceiver has direct access to the signal observed at each element. Near-field modeling and a performance analysis for multi-user extremely large scale MIMO was studied in [9], taking into account the variations of the signal amplitude and the projected aperture across the array elements.

One of the advantages of near-field beamforming is that it is possible to provide a certain degree of range discrimination. This distance discrimination allows the array to reduce the effects of reflected wavefronts arriving from the same angle of incidence but originating from different distances [10]. However, the potential of range discrimination of near-field beamforming has not been fully exploited from the communication perspective. Motivated by this fact, in this paper we exploit the range discrimination capability of near-field beamforming to facilitate the deployment of high-rate multi-user downlink MIMO mmWave systems. We consider the spectral efficiency achievable for a "worst case" scenario where the users are located at the same angular direction but with different distances. Additionally, we constrain the elements of the beamforming vectors to constant modulus, thus employing phase-only beamforming. The performance of the maximum ratio transmission (MRT), zero-forcing (ZF), minimum

mean squared error (MMSE), and leakage-based precoding schemes is investigated.

2. SYSTEM MODEL

We consider a downlink multi-user MIMO system where the BS is equipped with a uniform linear array (ULA) of M_{T} antennas, serving K user equipments (UEs) each with M_{R} antennas in the radiative near-field of the BS. The radiative near-field lies between the Fraunhofer distance ($d_F = \frac{2D^2}{\lambda}$) and the Fresnel distance ($d_N = \sqrt[3]{\frac{D^4}{8\lambda}}$), where D is the antenna diameter and λ is the wavelength [4].

For simplicity, we assume a 2-D setup and consider only the line-of-sight (LoS) path. We assume that d is the inter-element spacing for arrays at the BS and UE. The (x, y) coordinates of the n-th element of the BS array are given by

$$\boldsymbol{b}_n = \left[0, \left(n - \frac{M_{\mathrm{T}}-1}{2}\right) d\right]^{\mathsf{T}}, \; 0 \le n \le M_{\mathrm{T}} - 1. \tag{1}$$

The coordinate system is defined such that its origin is at the phase center of the BS array. Equally, the position vector for the m-th element of the k-th UE array is given as

$$\boldsymbol{u}_m^{(k)} = \left[\alpha_m^{(k)}, \beta_m^{(k)}\right]^{\mathsf{T}}, \; 0 \le m \le M_{\mathrm{R}} - 1, \tag{2}$$

where $\alpha_m^{(k)} = (m - \frac{M_{\mathrm{R}}-1}{2}) d \cos\phi_{\text{array}}^{(k)} + r^{(k)} \cos\phi_{\text{UE}}^{(k)}$ and $\beta_m^{(k)} = (m - \frac{M_{\mathrm{R}}-1}{2}) d \sin\phi_{\text{array}}^{(k)} + r^{(k)} \sin\phi_{\text{UE}}^{(k)}$. Furthermore, $\phi_{\text{array}}^{(k)}$ is the array orientation, $\phi_{\text{UE}}^{(k)}$ is the angle towards the UE from the BS, and $r^{(k)}$ is the distance towards the UE. Here we assume that the UE array is orthogonal to the line connecting the phase centers between the BS and UE arrays as depicted in Fig. 1. The received signal at the k-th UE is expressed as

$$\boldsymbol{y}_k = \boldsymbol{A}_k \boldsymbol{W}_k \boldsymbol{d}_k + \sum_{j=1, j\neq k}^{K} \boldsymbol{A}_k \boldsymbol{W}_j \boldsymbol{d}_j + \boldsymbol{z}_k \in \mathbb{C}^{M_{\mathrm{R}}}, \tag{3}$$

where $\boldsymbol{z}_k$ denotes additive white Gaussian noise with variance σ_n^2, $\boldsymbol{W}_k \in \mathbb{C}^{M_{\mathrm{T}} \times Q}$ is the precoding matrix for the kth UE, $\boldsymbol{d}_k \in \mathbb{C}^{Q}$ represents the data vector for the k-th UE, and Q is the number of streams for that particular UE. The matrix $\boldsymbol{A}_k$ which represents the channel between the BS and the k-th user is given as,

$$\boldsymbol{A}_k = \begin{bmatrix} a_{1,1}^{(k)} & a_{1,2}^{(k)} & \cdots & a_{1,M_{\mathrm{T}}}^{(k)} \\ a_{2,1}^{(k)} & a_{2,2}^{(k)} & \cdots & a_{2,M_{\mathrm{T}}}^{(k)} \\ \vdots & \ddots & \ddots & \vdots \\ a_{M_{\mathrm{R}},1}^{(k)} & a_{2,2}^{(k)} & \cdots & a_{M_{\mathrm{R}},M_{\mathrm{T}}}^{(k)} \end{bmatrix} \in \mathbb{C}^{M_{\mathrm{R}} \times M_{\mathrm{T}}}, \tag{4}$$

where $a_{m,n}^{(k)} = e^{-j2\pi \frac{\delta_{m,n}^{(k)}}{\lambda}}$ and $\delta_{m,n}^{(k)}$ is the path difference between the n-th element of the array at the BS and the m-th antenna of the k-th UE given as

$$\begin{aligned} \delta_{m,n}^{(k)} &= \|\boldsymbol{u}_m^{(k)} - \boldsymbol{b}_n\|_2 \\ &= \sqrt{\left(\alpha_m^{(k)}\right)^2 + \left(\beta_m^{(k)} - \left(n - \frac{M_{\mathrm{T}}-1}{2}\right) d\right)^2}. \end{aligned}$$

Note that the exact expression of the array steering vector depends on the path difference expression which is a function of the adopted wavefront model. Let us denote $\boldsymbol{A}$ and $\boldsymbol{W}$ as the system-wide steering and precoding block matrices, respectively defined as

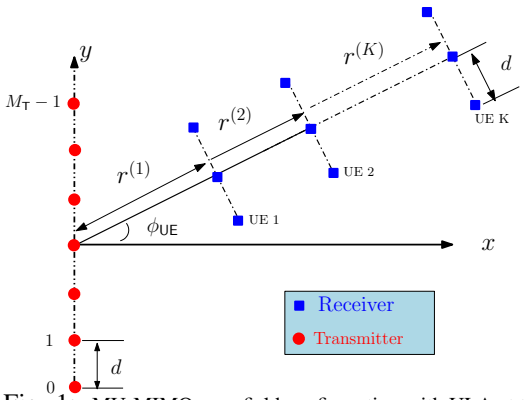

Fig. 1: MU-MIMO near-field configuration with ULA at the BS, $\phi_{\text{UE}}^{(1)} = \phi_{\text{UE}}^{(2)} = \cdots = \phi_{\text{UE}}^{(K)} = \phi_{\text{UE}}$

$$\boldsymbol{A} = [\boldsymbol{A}_1^{\mathsf{T}}, \boldsymbol{A}_2^{\mathsf{T}}, \cdots, \boldsymbol{A}_K^{\mathsf{T}}]^{\mathsf{T}} \in \mathbb{C}^{M_{\mathrm{R}}K \times M_{\mathrm{T}}} \tag{5}$$

$$\boldsymbol{W} = [\boldsymbol{W}_1, \boldsymbol{W}_2, \cdots, \boldsymbol{W}_K] \in \mathbb{C}^{M_{\mathrm{T}} \times QK}, \tag{6}$$

we normalize $\boldsymbol{W}$ such that $\|\boldsymbol{W}\|_{\mathrm{F}} = 1$. Additionally, we denote the multi-user interference channel block matrix relative to the k-th UE as

$$\tilde{\boldsymbol{A}}_k = [\boldsymbol{A}_1^{\mathsf{T}}, \cdots, \boldsymbol{A}_{k-1}^{\mathsf{T}}, \boldsymbol{A}_{k+1}^{\mathsf{T}}, \cdots, \boldsymbol{A}_K^{\mathsf{T}}]^{\mathsf{T}} \in \mathbb{C}^{M_{\mathrm{R}}(K-1) \times M_{\mathrm{T}}}. \tag{7}$$

As a performance metric we adopt the system-wide achievable rate, which is expressed as

$$R = \log_2 \det\left(\boldsymbol{I}_{M_{\mathrm{R}}K} + \frac{P}{M_{\mathrm{T}}\sigma_n^2} \boldsymbol{A}\boldsymbol{W}\boldsymbol{W}^{\mathsf{H}}\boldsymbol{A}^{\mathsf{H}}\right), \tag{8}$$

where P is the maximum power available at the BS. In the following, we consider several precoding schemes for the near-field beamforming in the multi-user mmWave communication systems to maximize the achievable rate. The elements of the overall beamforming matrix $\boldsymbol{W}$ are constrained to be constant modulus, thus representing phase-only beamforming.

3. PRECODING METHODS

In this section, we relax the constant modulus constraints on the precoding matrix and design the precoding matrix and thereafter project the resulting continuous-amplitude precoding matrix unto the unit circle. We consider the following two setups for the multi-user MIMO mmWave communication system.

3.1. MU-MISO transmision

In the first case, we assume a single antenna ($M_{\mathrm{R}} = 1$) at each of the K UEs. We consider near-field beamforming for the MU-MISO mmWave system using the following precoding methods.

3.1.1. Maximum Ratio Transmission

The maximum ratio transmission (MRT) precoder $\boldsymbol{w}_k^{\text{MRT}}$ is designed to maximize the received signal power at the desired UE [11]. It can be expressed as

$$\boldsymbol{w}_k^{\text{MRT}} = \arg\max_{\boldsymbol{w}} |\boldsymbol{w}_k^{\mathsf{H}} \boldsymbol{a}_k|^2 = \frac{\boldsymbol{a}_k}{\|\boldsymbol{a}_k\|_2}, \tag{9}$$

while the beamforming vector after constraining to only phases is denoted by

$$\boldsymbol{w}_{\text{CMC},k}^{\text{MRT}} = \text{Proj}\left(\boldsymbol{w}_k^{\text{MRT}}\right), \tag{10}$$

where $\text{Proj}(z_i) = \frac{z_i}{|z_i|}$ is the element-wise projection function. The vector $\boldsymbol{a}_k \in \mathbb{C}^{M_{\text{T}} \times 1}$ is a special case of the matrix $\boldsymbol{A}_k \in \mathbb{C}^{M_{\text{R}} \times M_{\text{T}}}$ assuming a single antenna at the k-th receiver, i.e., $(M_{\text{R}} = 1)$.

3.1.2. Zero-Forcing

The zero-forcing (ZF) scheme is given as

$$\boldsymbol{W}^{\text{ZF}} = \frac{\boldsymbol{A}^{+}}{\|\boldsymbol{A}^{+}\|_F}, \tag{11}$$

and the constrained beamforming as

$$\boldsymbol{W}_{\text{CMC}}^{\text{ZF}} \longleftarrow \text{Proj}\left(\boldsymbol{W}^{\text{ZF}}\right), \tag{12}$$

where $\boldsymbol{A}^{+}$ is the pseudo-inverse of $\boldsymbol{A}$. The ZF scheme enforces the zero MUI condition $\tilde{\boldsymbol{A}}_k \boldsymbol{w}_k^{\text{ZF}} = \boldsymbol{0}$ by basically forcing the $\boldsymbol{w}_k^{\text{ZF}}$ to lie in the null space of $\tilde{\boldsymbol{A}}_k$ so as to avoid the interference from user k to other users, where $\boldsymbol{w}_k^{\text{ZF}}$ denotes the kth column of $\boldsymbol{W}^{\text{ZF}}$. We assume that we implement a large antenna array at the BS, which means M_{T} is very large such that $M_{\text{T}} \gg K$ to ensure that the null space of $\tilde{\boldsymbol{A}}_k$ (i.e.,$\tilde{\boldsymbol{V}}_k^{(0)}$) exists. This solution results in good performance since it completely cancels the multi-user interference at every receiver. However, this solution is sensitive to unmodeled interference and other sources of distortion and may not result to the optimal signal-to-interference-plus-noise ratio. Moreover, choosing the precoding vector according to (11) imposes a strong condition on the system configuration in terms of the number of antennas that are needed [12].

3.1.3. Minimum Mean Square Error

The minimum mean square error (MMSE) scheme is a form of a regularized ZF process, which is seen as a solution to the noise enhancement problem of the ZF precoder. The precoder that minimizes the mean square error is given as

$$\boldsymbol{W}^{\text{MMSE}} = \frac{\bar{\mathbf{A}}}{\|\bar{\mathbf{A}}\|_F}, \tag{13}$$

$$\boldsymbol{W}_{\text{CMC}}^{\text{MMSE}} \longleftarrow \text{Proj}\left(\boldsymbol{W}^{\text{MMSE}}\right), \tag{14}$$

where $\bar{\boldsymbol{A}} = (\boldsymbol{A}^{\mathsf{H}}\boldsymbol{A} + \sigma_n^2 \boldsymbol{I}_{M_{\text{T}}})^{-1}\boldsymbol{A}^{\mathsf{H}}$.

3.1.4. Leakage-Based Precoder

The *leakage*-based precoder is designed to maximize the signal-to-leakage-noise ratio (SLNR) defined as

$$\Omega_k = \frac{|\boldsymbol{w}_k^{\mathsf{H}} \boldsymbol{a}_k|^2}{\|\tilde{\boldsymbol{A}}_k \boldsymbol{w}_k\|^2 + \sigma_k^2}. \tag{15}$$

Maximizing the SLNR for all the users is an efficient way of designing the transmit precoding vectors because it limits the search space and also lowers the complexity involved in finding efficient transmit precoders [13]. According to the generalized Rayleigh-Ritz quotient method [14], the optimal $\boldsymbol{w}_k^{\text{SLNR}}$ is given as

$$\boldsymbol{w}_k^{\text{SLNR}} = \boldsymbol{v}_{\max}\left(\left(\tilde{\boldsymbol{A}}_k^{\mathsf{H}}\tilde{\boldsymbol{A}}_k + \sigma_n^2 \boldsymbol{I}_{M_{\text{T}}}\right)^{-1} \boldsymbol{a}_k \boldsymbol{a}_k^{\mathsf{H}}\right), \tag{16}$$

$$\boldsymbol{w}_{\text{CMC},k}^{\text{SLNR}} \longleftarrow \text{Proj}\left(\boldsymbol{w}^{\text{SLNR},k}\right), \tag{17}$$

where $\boldsymbol{v}_{\max}\{\cdot\}$ is the eigenvector corresponding to the largest eigenvalue of the matrix.

3.2. MU-MIMO transmission

Next, we consider the general MU-MIMO setup and use all the above precoding methods. In addition, we use the block diagonalization (BD) scheme for the cancellation of the MUI. The BD scheme is a more generalized ZF solution applicable for a scenario when the receiver has multiple antennas [12]. The BD scheme enforces the following zero MUI condition $\tilde{\boldsymbol{A}}_k \boldsymbol{W}_k = \boldsymbol{0}$, which can be expressed as

$$\boldsymbol{W}_k^{\text{BD}} = \tilde{\boldsymbol{V}}_k^{(0)} \boldsymbol{V}_k^{\max}, \tag{18}$$

$$\boldsymbol{W}_{\text{CMC},k}^{\text{BD}} \longleftarrow \text{Proj}\left(\boldsymbol{W}^{\text{BD},k}\right), \tag{19}$$

where $\tilde{\boldsymbol{V}}_k^{(0)}$ holds the basis for the null-space of $\tilde{\boldsymbol{A}}_k$, which can be obtained from the singular value decomposition (SVD) of $\tilde{\boldsymbol{A}}_k$ [12] and $\boldsymbol{V}_k^{\max}$ is a matrix whose columns are the right singular vectors corresponding to the M_{R} largest singular values of $\boldsymbol{A}_k \tilde{\boldsymbol{V}}_k^{(0)}$.

4. NUMERICAL RESULTS

In this section, we show simulation results to evaluate the performance of the transmit precoding methods considered for the near-field beamforming for MU-MIMO mmWave systems. We assume that the BS uses ULA with $M_{\text{T}} = 128$ antennas which are uniformly spaced with $d = \lambda/2$ at a carrier frequency of 28 GHz. We consider a system with $\sigma_n^2 = 1$ and $K = 5$ UEs each with $M_{\text{R}} = 4$ antennas. We present a worst-case scenario where the UEs are uniformly spaced at the same angle in the radiative near-field of the BS antenna as shown in Fig. 1. We assume that the UEs have the same AoA $\theta_1 = \theta_K = 90^\circ$ where the angle is with respect to the phase center of the BS array.

Fig. 2a shows the normalized beam pattern for the MRT scheme for the different users versus their distance from the

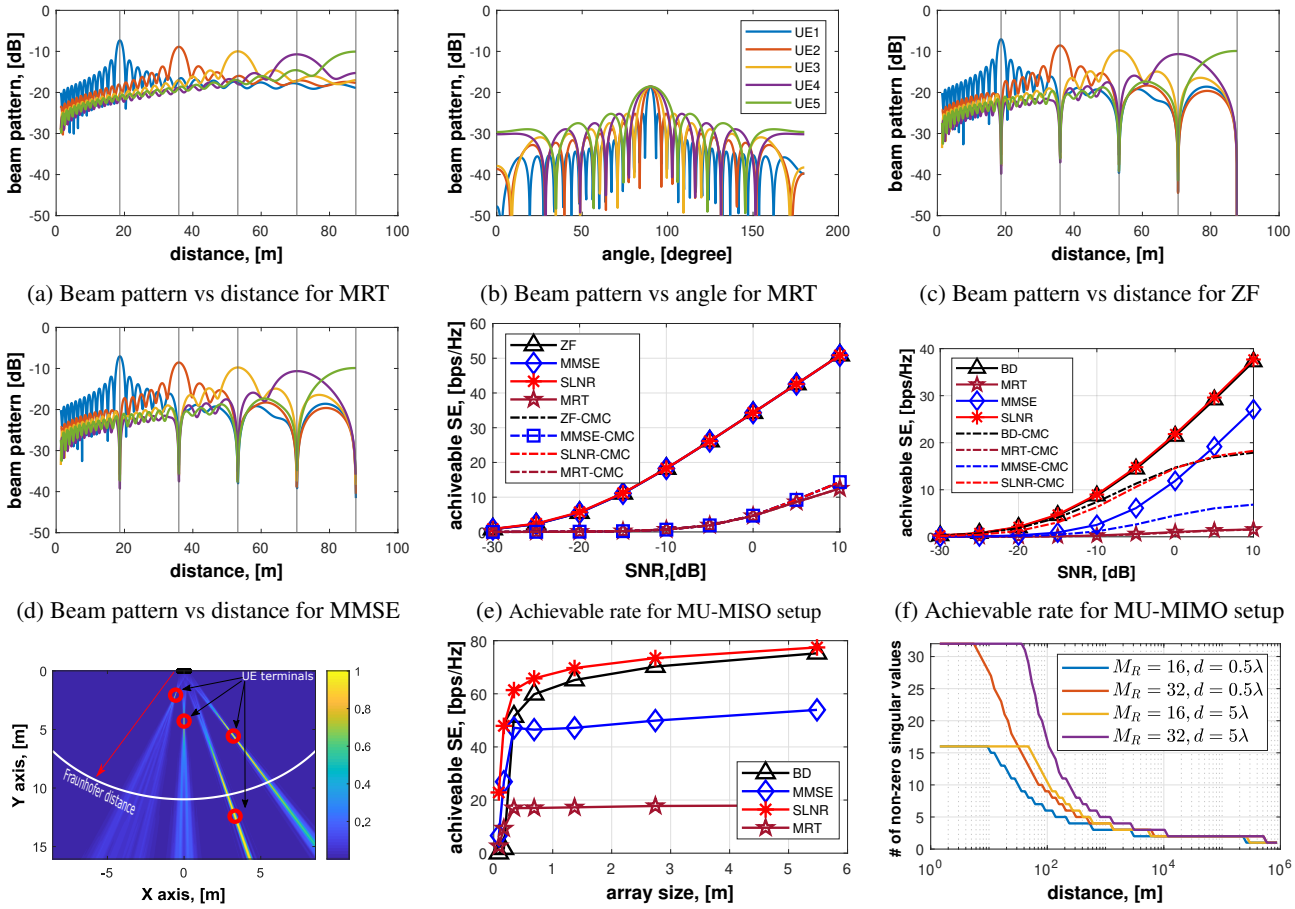

(a) Beam pattern vs distance for MRT

(b) Beam pattern vs angle for MRT

(c) Beam pattern vs distance for ZF

(d) Beam pattern vs distance for MMSE

(e) Achievable rate for MU-MISO setup

(f) Achievable rate for MU-MIMO setup

(g) Beamfocus for MU-MIMO

(h) Achievable rate vs array size

(i) Non-zero Singular Values vs distance

Fig. 2: Simulation results

transmitting antenna for the MU-MISO setup. The result depicts the distance discrimination potentials of the near-field beamforming, as the UEs can be separated by their respective distance to the BS. It is seen that the MRT schemes do not cancel the MUI and that the UE closer to the BS has a more focused beam, while the beam focus expands for UEs farther away from the BS. Furthermore, Fig. 2b depicts the normalized beam pattern with the AoA of $\theta = 90^\circ$ for all the UEs, with the range $\theta \in [0^\circ, 180^\circ]$. It is observed that similar to the previous result the UE farthest from the BS has directivity similar to the far-field scenario, while the closet UE has the best directivity.

In Fig. 2c and 2d we show the normalized beam pattern versus distance for the ZF and MMSE schemes for the MU-MISO setup, respectively. Both precoding schemes improve the performance of the system by canceling the multi-user interference and improving the directivity of the beam for the desired users. Moreover, Fig. 2e shows the achievable rate for the MU-MISO setup for different signal-to-noise ratios (SNRs). It is observed that the MRT scheme has the worst performance as it does not attempt to cancel the MUI in the system. Furthermore, we observe comparable performance improvement with respect to the achievable rate for the other considered precoding schemes. The MMSE scheme depends on the levels of interference and noise: in the case that SNR is low, then the MMSE scheme looks more like an MRT, and in the case that SNR is high, then the MMSE scheme looks more like a ZF scheme.

In Fig. 2f, the achievable rate for the MU-MIMO setup is evaluated with respect to different values of SNR. The SLNR scheme outperforms other schemes in the high SNR regime, while the BD scheme has a better performance than the MMSE scheme because the BD scheme has the ability to make optimal use of the excess degrees of freedom available at the transmitter. We observe that there is a performance degradation between the continuous-amplitude solution and the constant modulus (CMC) solution.

In Fig. 2g, we show the distance discriminating potential of the near-field beamforming, with the normalized signal power of the transmitted signal to each UE at the various UE locations within the near-field of the BS antenna. It is observed from the figure that the maximum normalized signal power is realized around the location of each UE. This shows that near-field beamforming allows the concurrent transmission to multiple UEs at various distances located at the same angular direction. This is one of the major distinguishing fea-

tures of near-field beamforming from conventional far-field beamforming.

Furthermore, Fig. 2h depicts the achievable rate for the MU-MIMO setup with respect to increasing array size, which is given as $M_{\mathrm{T}}d$. We consider various values of M_{T} with a fixed $d = \lambda/2$ assuming the SNR is 20 dB. It is observed that the achievable spectral efficiency improves with an increase in the array size for the considered precoding schemes with the MRT having the worst performance.

In Fig. 2i, we show the profile of the number of non-zero singular values of the steering matrix as a function of distance for the various combinations of the number of antennas at the UE and inter-element spacing, d. From the figure, we observe that spatial multiplexing is possible in the near-field, and that the number of streams Q that can be transmitted to a UE is dependent on distance. The range of distances for the maximum possible streams (full rank) is increased with an increase in the aperture of the antenna array.

5. CONCLUSIONS

In this paper, we have exploited the distance discrimination potential of the near-field beamforming from communication perspective to facilitate the deployment of high-rate MU-MIMO millimeter wave systems. We studied the performance of the system with the MRT, ZF, MMSE, and SLNR precoding schemes. Simulation results showed that for the MU-MIMO setup, the SLNR scheme performs better than the other schemes. The block diagonalization (BD) scheme, which is a generalized ZF scheme, has improved performance than the MMSE due to the ability of the BD to make optimal use of the excess degrees of freedom available at the BS.

Acknowledgments

This work was supported by Nnamdi Azikiwe University Nigeria, under NEEDS Assessment Fund and the Communication Research Laboratory, Ilmenau University of Technology, Germany.

6. REFERENCES

[1] J. G. Andrews, S. Buzzi, W. Choi, S. V. Hanly, A. Lozano, A. C. K. Soong, and J. C. Zhang, "What will 5G be?" *IEEE Journal on Selected Areas in Communications*, vol. 32, no. 6, pp. 1065–1082, 2014.

[2] J. Zhang, E. Björnson, M. Matthaiou, D. W. K. Ng, H. Yang, and D. J. Love, "Prospective multiple antenna technologies for beyond 5G," *IEEE Journal on Selected Areas in Communications*, vol. 38, no. 8, pp. 1637–1660, 2020.

[3] K. T. Selvan and R. Janaswamy, "Fraunhofer and fresnel distances : Unified derivation for aperture antennas." *IEEE Antennas and Propagation Magazine*, vol. 59, no. 4, pp. 12–15, 2017.

[4] H. Zhang, N. Shlezinger, F. Guidi, D. Dardari, M. F. Imani, and Y. C. Eldar, "Beam focusing for near-field multiuser MIMO communications," *IEEE Transactions on Wireless Communications*, vol. 21, no. 9, pp. 7476–7490, 2022.

[5] F. Guidi and D. Dardari, "Radio positioning with em processing of the spherical wavefront," *IEEE Transactions on Wireless Communications*, vol. 20, no. 6, pp. 3571–3586, 2021.

[6] K. Nishimori, N. Honma, T. Seki, and K. Hiraga, "On the transmission method for short-range MIMO communication," *IEEE Transactions on Vehicular Technology*, vol. 60, no. 3, pp. 1247–1251, 2011.

[7] A. d. J. Torres, L. Sanguinetti, and E. Björnson, "Near- and far-field communications with large intelligent surfaces," *arXiv preprint arXiv: 2011.13835*, 2020. [Online]. Available: https://arxiv.org/abs/2011.13835

[8] W. Tang, M. Z. Chen, X. Chen, J. Y. Dai, Y. Han, M. Di Renzo, Y. Zeng, S. Jin, Q. Cheng, and T. J. Cui, "Wireless communications with reconfigurable intelligent surface: Path loss modeling and experimental measurement," *IEEE Transactions on Wireless Communications*, vol. 20, no. 1, pp. 421–439, 2021.

[9] H. Lu and Y. Zeng, "Near-field modeling and performance analysis for multi-user extremely large-scale MIMO communication," *IEEE Communications Letters*, vol. 26, no. 2, pp. 277–281, 2022.

[10] R. Liu and K. Wu, "Antenna array for amplitude and phase specified near-field multifocus," *IEEE Transactions on Antennas and Propagation*, vol. 67, no. 5, pp. 3140–3150, 2019.

[11] E. Björnson, M. Bengtsson, and B. Ottersten, "Optimal multiuser transmit beamforming: A difficult problem with a simple solution structure [lecture notes]," *IEEE Signal Processing Magazine*, vol. 31, no. 4, pp. 142–148, 2014.

[12] Q. H. Spencer, A. L. Swindlehurst, and M. Haardt, "Zero-forcing methods for downlink spatial multiplexing in multiuser MIMO channels," *IEEE Transactions on Signal Processing*, vol. 52, no. 2, pp. 461–471, 2004.

[13] M. Sadek, A. Tarighat, and A. H. Sayed, "A leakage-based precoding scheme for downlink multi-user MIMO channels," *IEEE Transactions on Wireless Communications*, vol. 6, no. 5, pp. 1711–1721, 2007.

[14] G. H. Golub and C. F. Van Loan, *Matrix computation*. Johns Hopkins University Press, 2013.